Hybrid functional study of band structures of $GaAs_{1-x}N_x$ and $GaSb_{1-x}N_x$ alloys

Ville Virkkala, Ville Havu, Filip Tuomisto, and Martti J. Puska
Department of Applied Physics, Aalto University, P.O. Box 11100, FI-00076 Aalto, Finland
(Received 18 August 2011; revised manuscript received 8 November 2011; published 29 February 2012)

Band structures of $GaAs_{1-x}N_x$ and $GaSb_{1-x}N_x$ alloys are studied in the framework of the density functional theory within the hybrid functional scheme (HSE06). We find that the scheme gives a clear improvement over the traditional (semi)local functionals in describing, in a qualitative agreement with experiments, the bowing of electron energy band gap in $GaAs_{1-x}N_x$ alloys. In the case of $GaSb_{1-x}N_x$ alloys, the hybrid functional used makes the study of band structures possible *ab initio* without any empirical parameter fitting. We explain the trends in the band gap reductions in the two materials that result mainly from the positions of the nitrogen-induced states with respect to the bottoms of the bulk conduction bands.

DOI: 10.1103/PhysRevB.85.085134 PACS number(s): 71.20.Nr, 71.55.Eq, 71.15.Mb, 61.72.uj

I. INTRODUCTION

During the past two decades there have been many experimental and computational studies considering dilute III-V nitrides (for reviews, see Refs. 1 and 2). The interest stems from the fact that replacing the V component by just a small fraction of nitrogen, having a small covalent radius and high electronegativity, strongly modifies the conduction band structure of the III-V compound. Opposite to the expectations arising from large nitride band gaps, the band gaps in dilute nitride alloys decrease with increasing nitrogen concentration and the reduction is much stronger than a linear dependence. The effects cannot be explained, e.g., by the virtual crystal approximation. Moreover, the electron effective mass at the conduction band edge attains abnormally high values. Archetypal examples are the $GaAs_{1-x}N_x$ alloys that show band gap reduction with increasing nitrogen concentration $x < 0.03$ (see Ref. 3). The effect of nitrogen is even more dramatic in $GaSb_{1-x}N_x$ alloys with the maximum electronegativity difference between two group-V species.[4–6] This kind of tunability of the band gap is considered to enable new optoelectronic applications.[7]

In many cases, the experimentally observed band gap bowing due to nitrogen can be roughly described by using the band anticrossing (BAC) model.[8] One central assumption behind the BAC model is that nitrogen induces a localized resonant state above the conduction band edge of the host material. The resonant state interacts with the host material states and pushes the conduction band edge lower causing a band gap reduction. A fact complicating the picture with respect to the simple BAC model is that randomly formed nitrogen clusters can form a spectrum of N-related states. This was realized on the basis of large-supercell calculations[9,10] and the existence of nitrogen pairs has been since seen in cross-sectional scanning tunneling images and in the corresponding differential conductance spectra proportional to the local density of states.[11]

The effect of nitrogen on III-V nitrides has been successfully described by tight-binding (TB) calculations.[12,13] Especially the method[10] in which the conduction band edge is represented as a linear combination of isolated nitrogen resonant states (LCINS) and the host material conduction band edge wave functions can take the nitrogen clustering into account.[2,11] Another view on the band gap bowing in III-V nitrides is provided by the empirical pseudopotential method.[9] In contrast to the BAC model, the results of empirical pseudopotential calculations emphasize that the modification of the bottom of the conduction band is due to nitrogen-induced mixing of the conduction band valley states. The tight-binding and empirical pseudopotential methods enable the use of large supercells (up to thousands of atoms) in the simulations and therefore the random distribution of nitrogen in the alloy, including the possible formation of nitrogen clusters, can be statistically modeled.

In this work, we consider $GaAs_{1-x}N_x$ and $GaSb_{1-x}N_x$ alloys. Our main interest is in the $GaSb_{1-x}N_x$ alloys which show, due to the direct, relatively small band gaps, a large potential in fabricating long-wavelength lasers. For $GaAs_{1-x}N_x$, a large number of experimental and theoretical studies exists and therefore the alloy serves as an important test case for our modeling. When the effect of nitrogen on $GaSb_{1-x}N_x$ alloys is considered, $GaAs_{1-x}N_x$ also serves as an important point of comparison from the viewpoint of the role of localized Ga-N bond states in the two materials. For example, according to photoluminescence measurements, nitrogen forms resonant levels above the bottom of the conduction band in $GaAs_{1-x}N_x$[14] whereas tight-binding calculations suggest that in $GaSb_{1-x}N_x$ alloys nitrogen-induced levels lie near or below the bottom of the conduction band.[15]

We model the alloys by first-principles density-functional electronic structure calculations within the supercell approximation. In contrast to the tight-binding and empirical pseudopotential methods, our approach can treat only much smaller supercells (up to hundreds of atoms). On the other hand, the first-principles calculations have indisputable predictive power for the nitrogen-induced changes in the electronic structure. Specially, due to the localized character of the induced states, it is important that the electronic structure is solved self-consistently, including the ionic relaxation.

First-principles density-functional theory (DFT) electronic structure calculations have been used to model nitrogen in $GaAs_{1-x}N_x$ alloys and also to a smaller extent in $GaSb_{1-x}N_x$ alloys. Interstitial nitrogen in GaAs has been considered in several studies.[16–18] Lowther *et al.*[19] discussed the relative importance of different nitrogen defects, especially that of the N_2 dimer on the As site and the substitutional N on the Ga site, in GaAs on the basis of the calculated formation

 ©2012 American Physical Society

energies. Laaksonen *et al.*[20] studied the effects of substitutional nitrogen pairs on the GaAs band structure and the density of states. Belabbes *et al.*[21] predicted the decrease of the band gap in $GaSb_{1-x}N_x$ as a function of the nitrogen concentration in agreement with experimental findings.

The above-mentioned density-functional studies have been performed within the local or semilocal approximation for the electron exchange and correlation, i.e., using the local density approximation (LDA) or the generalized gradient approximation (GGA). The drawback of these methods is a substantial underestimation of energy band gaps. This makes the modeling of the effects of nitrogen cumbersome because of the uncertainty of the defect level positions with respect to the band edges; even the character, localized or delocalized, of the defect state may be incorrectly described. Belabbes *et al.*[21] corrected for the too small band gap by an empirical shift. In contrast, in the present work, we make use of hybrid functionals,[22] in which part of the semilocal exchange-correlation functional is substituted by the Hartree-Fock exchange. Hybrid functionals give band gaps near to the experimental ones. They are computationally clearly more expensive than semilocal functionals, but afford calculations with supercells up to around 200 atoms.

In the present work, we consider substitutional nitrogen impurities at anion sites and corresponding impurity pairs in $GaAs_{1-x}N_x$ and $GaSb_{1-x}N_x$ alloys. Moreover, we include in our studies also nitrogen dimers occupying a single anion site. The results show how different types of nitrogen configurations affect the host band structure. Specially, we find that besides the distance between the nitrogen atoms in a pair, also their orientation in the lattice plays an important role in their effect on the band structure. In addition, in the case of $GaSb_{1-x}N_x$ and assuming no nitrogen clustering, we calculate systematically the dependence of the band gap on the nitrogen concentration.

II. METHODS AND STUDIED SYSTEMS

All calculations were performed using the Vienna *ab initio* simulation package (VASP)[23] with the projector augmented wave (PAW)[24] method and the HSE06 hybrid functional.[22] The HSE06 hybrid functional replaces the DFT exchange by the exact Hartree-Fock (HF) counterpart only within the rapidly-decaying regime.[22] This feature makes it computationally faster and more reliable than hybrid functionals that use the exact HF exchange.[22] For the HF mixing constant α, we used the default value of 0.25. We chose this value because it can be justified analytically using perturbation theory[25] and we wanted to avoid empirical parameter fitting. For the HSE range separation parameter μ, we used the value $\mu = 0.2/\text{Å}$. The kinetic energy cutoff of 400 eV was used for the plane-wave basis of wave functions, which gives a reasonable convergence of the total energy in both materials. The uppermost d electrons, including the Ga $3d$ electrons, were treated as core. All studied configurations were charge neutral. We did not take spin-orbit splitting into account in our calculations. In GaSb, spin-orbit splitting is reported to decrease the band gap about 0.24 eV by raising the top of the valence band.[26,27] Because the spin-orbit splitting occurs mainly in the top of the valence band, the qualitative effects to our calculations are minor.

In the case of $GaAs_{1-x}N_x$, we studied five different configurations: the single nitrogen atom $[Ga_{32}As_{31}N_{As}]$ and N_2 dimer $[Ga_{32}As_{31}(N_2)_{As}]$ on the substitutional As site in the supercell of 64 atoms and three configurations of two nitrogen atoms located on two separate substitutional As sites. These three configurations were in the supercell of 64 atoms: (i) as far as possible corresponding to the (1,1,1) a lattice vector $[Ga_{32}As_{30}(N_{As}N_{As})_{far}]$, where a is the cubic lattice parameter, (ii) as near as possible corresponding to the (0.5,0.5,0) a lattice vector $[Ga_{32}As_{30}(N_{As}N_{As})_{near}]$, and (iii) at sites corresponding to the (1,0,0) a lattice vector $[Ga_{32}As_{30}(N_{As}N_{As})_{100}]$. The $2 \times 2 \times 2$ Monkhorst-Pack set was used for the **k**-point sampling in all cases. In the case of a single substitutional nitrogen atom, atoms were relaxed to their ground-state positions from their ideal positions retaining the initial tetrahedral symmetry during relaxation. In the case of two nitrogen atoms, atoms were relaxed to their ground-state positions without any symmetry restrictions. The stopping criterion for ionic relaxation in all cases was that total forces acting on each atom were smaller than 0.01 eV/Å. For each configuration, the lattice parameter was optimized using the relaxed atomic structure and finding the energy minimum with respect to the lattice parameter. The N_2 dimer case was calculated as spin polarized and the other cases spin compensated.

In the case of GaSb, we studied the same configurations as in the case of GaAs and the calculations were performed in a similar way. In addition, in the case of GaSb, the band gap was studied as a function of nitrogen concentration, with systems of bulk GaSb and one nitrogen atom in 64, 128, and 216-atom supercells, corresponding to 3.1%, 1.6%, and 0.9% nitrogen concentrations, respectively. In the case of the 128-atom supercell, the relaxation of ion positions and the lattice parameter optimization were performed similarly as in the other single nitrogen cases. However, in the case of the 216-atom supercell, the lattice parameter was interpolated using the lattice parameters of the smaller $GaSb_{1-x}N_x$ cells with higher nitrogen concentration and that of bulk GaSb and assuming a linear dependence between the lattice parameter and the nitrogen concentration. The relaxation of ionic positions was not performed either, but instead relaxed coordinates from the 64-atom supercell were placed into the 216-atom supercell. The band gap was calculated only at the Γ point using the HSE06 functional and Γ point approximation in the self-consistent electronic structure calculation. Band structures were not calculated in the case of larger supercells, due to the high computational cost of hybrid functionals when many **k**-points are used.

III. RESULTS

In the following two sections the band structures calculated for $GaAs_{1-x}N_x$ and $GaSb_{1-x}N_x$ systems are shown. In addition, the lattice parameters a, band gaps E_g, and relative binding energies $E_{b,\text{rel}}$ of two nitrogen atoms in different nitrogen configurations are given. The results are analyzed in more detail in the $GaSb_{1-x}N_x$ section also for $GaAs_{1-x}N_x$.

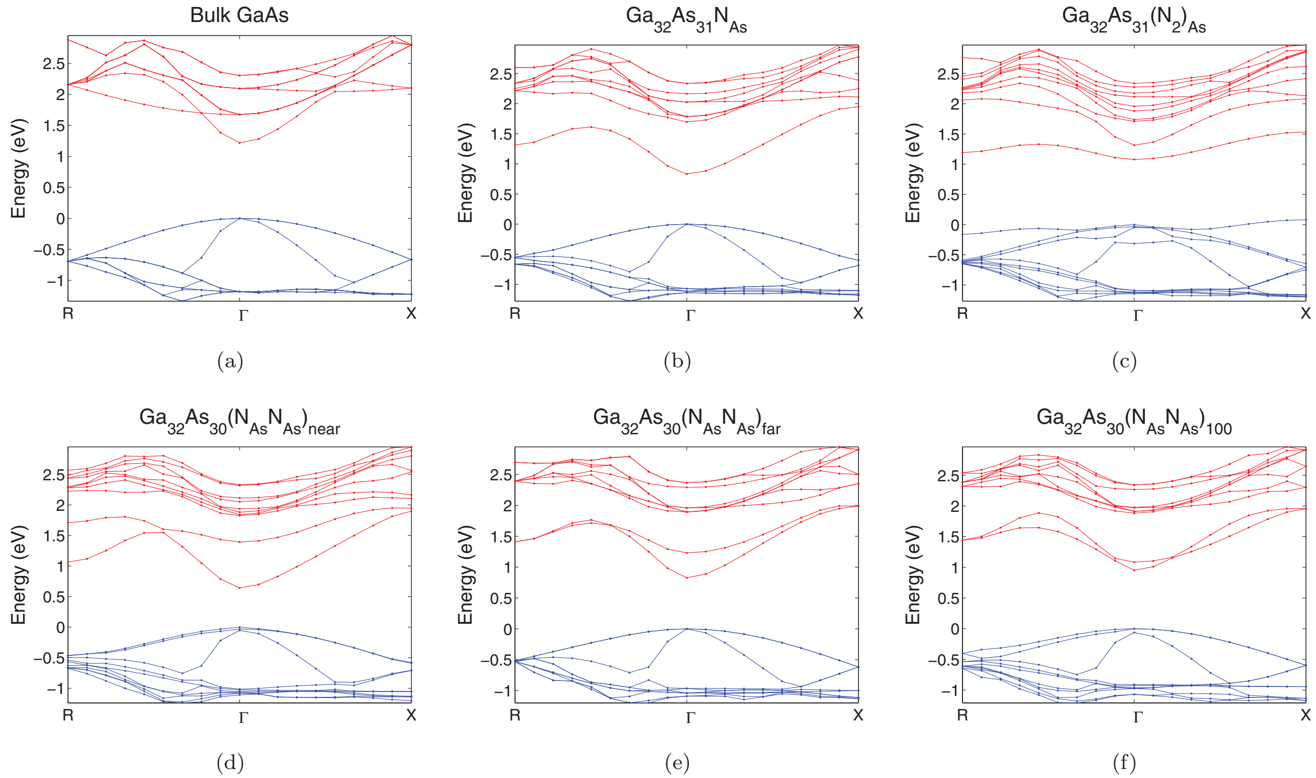

FIG. 1. (Color online) Band structures for the supercells of (a) bulk $Ga_{32}As_{32}$, (b) $Ga_{32}As_{31}N_{As}$ (c) $Ga_{32}As_{31}(N_2)_{As}$, (d) $Ga_{32}As_{30}(N_{As}N_{As})_{near}$, (e) $Ga_{32}As_{30}(N_{As}N_{As})_{far}$, and (f) $Ga_{32}As_{30}(N_{As}N_{As})_{100}$. The energy zero is defined to coincide with the top of the valence band.

A. $GaAs_{1-x}N_x$

Figure 1 shows the band structures of $GaAs_{1-x}N_x$ systems corresponding to different nitrogen configurations within 64-atom supercells, while Table I gives the corresponding lattice parameters, the relative binding energies, and the band gaps in different cases.

The binding energy of two nitrogen atoms relative to the case of two infinitely separated atoms is estimated, for example, for the $Ga_{32}As_{30}(N_{As}N_{As})_{far}$ case as

$$E_{b,\mathrm{rel}} = 2E[Ga_{32}As_{31}N_{As}] - E[Ga_{32}As_{30}(N_{As}N_{As})_{far}] - E[\mathrm{bulk}[Ga_{32}As_{32}]]. \quad (1)$$

In the case of $Ga_{32}As_{31}(N_2)_{As}$, we need to use reaction $2(Ga_{32}As_{31}N_{As}) + As \rightarrow Ga_{32}As_{31}(N_2)_{As} + Ga_{32}As_{32}$, i.e, add the chemical potential μ_{As} of As into Eq. (1) to get an energy comparable to other configurations. In As-rich growth conditions, μ_{As} equals to $\mu_{As(bulk)}$ and in Ga-rich growth conditions μ_{As} is obtained as $\mu_{As} = \mu_{GaAs} - \mu_{Ga}$, where μ_{Ga} equals to $\mu_{Ga(bulk)}$ and μ_{GaAs} is the energy of a two-atom unit of bulk GaAs.[28] The chemical potentials for bulk Ga and As are calculated in their respective geometries, which are *Cmca* for Ga and $R\bar{3}m$ for As. The obtained limits for μ_{As} are -7.00 eV $\leqslant \mu_{As} \leqslant -6.10$ eV corresponding to Ga-rich and As-rich growth conditions, respectively. The relative binding energy for $Ga_{32}As_{31}(N_2)_{As}$ in Table I is given in As-rich growth conditions. Above, the calculated total PAW energies E of the different supercells indicated in the brackets are used. This is not a very accurate way to compare binding energies of nitrogen atoms in different configurations, because the lattice parameters may differ, but it still gives good trends between different systems.

TABLE I. Relative binding energies $E_{b,\mathrm{rel}}$, lattice parameters a, and band gaps E_g of different nitrogen pair configurations in relaxed supercells for $GaAs_{1-x}N_x$ alloys.

Configuration	$E_{b,\mathrm{rel}}$ (eV)	a (Å)	E_g (eV)
bulk $Ga_{32}As_{32}$	...	5.70	1.22
$Ga_{32}As_{31}N_{As}$	...	5.66	0.83
$Ga_{32}As_{31}(N_2)_{As}$	−0.40	5.68	1.08
$Ga_{32}As_{30}(N_{As}N_{As})_{near}$	−0.02	5.62	0.64
$Ga_{32}As_{30}(N_{As}N_{As})_{far}$	0.35	5.62	0.83
$Ga_{32}As_{30}(N_{As}N_{As})_{100}$	0.26	5.62	0.95

For the band gap of bulk GaAs, we obtain the value of 1.22 eV, which is in good agreement with 1.21 eV given in the hybrid functional study of Ref. 22, but clearly less than 1.33 eV, given in Ref. 29 obtained also using hybrid functionals. However, in Ref. 29, also the Ga 3*d* electrons were treated as valence and the spin-orbit coupling effects were taken into account. The experimental value extrapolated to 0 K is 1.52 eV.[30] Thus our calculations underestimate the band gap by 20%, but it is much better than band gaps obtained using local or semilocal functionals that produce band gaps of around 0.5 eV.[17,20] The obtained lattice parameter for bulk GaAs is 5.70 Å (the Ga-As bond length is 2.47 Å). According to Table I, the calculated lattice parameters decrease with increasing

nitrogen concentration, which is in qualitative agreement with experiments.[31] However, typical for hybrid-functionals, the calculated lattice parameter is somewhat overestimated.

Comparison of the relative binding energies of different nitrogen configurations shows that in thermal equilibrium the formation of the N_2 dimer in the substitutional As site $[Ga_{32}As_{31}(N_2)_{As}]$ is unlikely even in As-rich growth conditions. For substitutional nitrogen atoms on As sites, it is energetically more favorable to be somewhat apart from each other and thus the equilibrium thermodynamics does not favor the formation of nitrogen pairs. The reason for this is that although the total energy can be lower when two defects share their surrounding shear fields, two nitrogen atoms being too near to each other causes larger structural changes into the host crystal than being somewhat more apart.

According to Fig. 1(b), the lowest conduction band separates in the case of a single substitutional nitrogen atom from the higher bands and the band gap is reduced from 1.22 to 0.83 eV. A reduction of 39% in the volume of the Ga tetrahedron surrounding the nitrogen atom is found. The Ga-N bond length is 2.08 Å, i.e., it becomes close to 1.97 Å for bulk GaN obtained using the HSE06 functional in the zinc blende structure. According to the density of states (DOS) shown in Fig. 2(a), nitrogen induces well localized states 1.7 eV above the valence band maximum (VBM). The fact that these states are related to the nitrogen atom can be deduced from the local density of states (LDOS) at the nitrogen atom (this is shown below in Fig. 4 for $Ga_{32}Sb_{31}N_{Sb}$).

In the case of the $Ga_{32}As_{31}(N_2)_{As}$ supercell, a rather small reduction in the band gap from 1.22 to 1.08 eV is observed and there is a reduction of 13% in the volume of the Ga tetrahedron surrounding the dimer. In Ref. 17, a rather similar calculation was done using the LDA with the PAW method considering an interstitial N_2 dimer in the center of a Ga tetrahedron. That calculation gave a reduction of only about 30 meV in the band gap. According to Fig. 1(c), the lowest conduction band becomes clearly separate from the other conduction bands and it is only slightly dispersed. In Ref. 17, this kind of adjustment of conduction bands was not observed. Thus it seems that on the interstitial site the N_2 dimer affects much less the electronic structure of the host material than on the substitutional site. According to the LDOS, at the nitrogen atoms, the lowest conduction band clearly results from the strong interaction between *p* electrons of the two nitrogen atoms, which have a localized state 1.18 eV above the VBM. The separation of the substitutional N_2 dimer related band is in accord with the LDA results of Ref. 19, but now this band is more dispersive and close to the conduction band minimum (CBM) instead of being a very deep midgap state. Thus our result does not support the idea of Ref. 19 that the dimer state reduces strongly the band gap.

In the case of two substitutional nitrogen atoms in the near configuration in the 64-atom supercell [see Fig. 1(d)], the band gap is reduced more than in the case of a single substitutional nitrogen atom, i.e., from 1.22 to 0.64 eV. There is a 37% reduction in the volume of the Ga tetrahedron surrounding each nitrogen atom, i.e., the reduction is quite similar to the case of a single substitutional nitrogen atom. According to the DOS in Fig. 2(a), the nitrogen related state is split into two in the near configuration. When the nitrogen atoms are

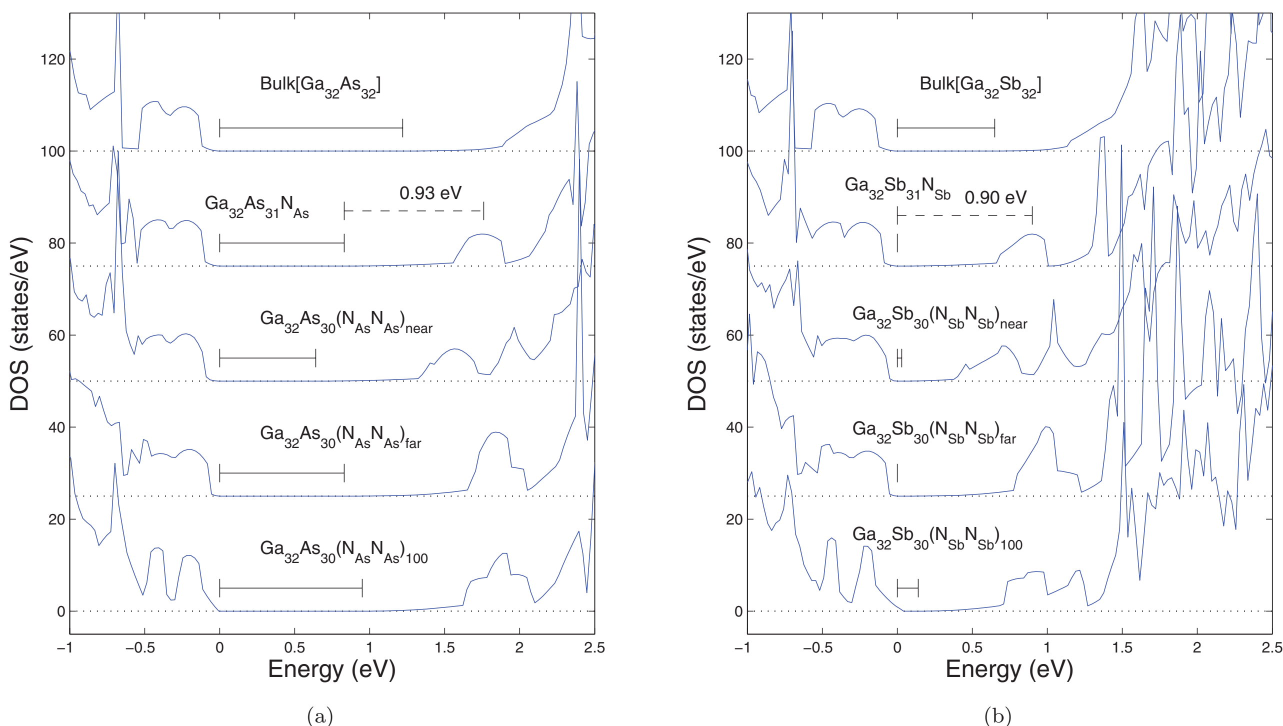

FIG. 2. (Color online) DOS in different nitrogen configurations in (a) $GaAs_{1-x}N_x$ and (b) $GaSb_{1-x}N_x$. The solid segments indicate the band gaps in different configurations and the dashed segments in the single nitrogen cases show the distance between the CBM and the nitrogen related states. The dashed lines show the zero level of DOS in different cases. The numbers on the vertical axes serve only as a scale.

in the far configuration, the band gap is in practice the same as in the single nitrogen case, although the bottom of the conduction band is split [see Fig. 1(e)]. Also the geometry, in which the nitrogen atoms are located in the centers of two Ga tetrahedra, resembles the isolated substitutional nitrogen case. In the (100) configuration, the band gap increases from 0.83 to 0.95 eV compared to the far configuration, even though the atomic structures are nearly identical and there is a 39% reduction in the volume of the Ga tetrahedron surrounding the nitrogen atoms in both configurations. According to the DOS, both in the far and (100) configurations in Fig. 2(a), the nitrogen atoms induce localized states 1.8 eV above the VBM. However, in the far configuration, the nitrogen-related peak in DOS seems to be narrower and thus the corresponding states are better localized than in the (100) configuration. The Ga-N bond lengths are very similar in all configurations, i.e., they are 2.07, 2.06, and 2.05 Å for the far, (100), and near configurations, respectively.

In a recent experimental study,[11] the band gap of GaAs was found to decrease from 1.42 to 1.20 eV, corresponding to a nitrogen concentration of 1.2% and thus our result for a single substitutional nitrogen atom in a 64-atom supercell, i.e., for the nitrogen concentration of 3.1%, seems to be in qualitative agreement with experimental values. In Ref. 11, it was observed, based on cross-sectional scanning tunneling microscopy, that the nitrogen atoms are not homogeneously distributed and local pairs of nitrogen atoms and also larger nitrogen agglomerates occur. Interestingly, according to our calculations, in the case of two nitrogen atoms, and a twice as high nitrogen concentration of 6.2%, the band gap does not systematically decrease compared to the single nitrogen case.

B. $GaSb_{1-x}N_x$

Figure 3 shows the calculated band structures for different $GaSb_{1-x}N_x$ configurations in the 64-atom supercell and Table II gives the corresponding relative binding energies, band gaps, and lattice parameters. The binding energies are calculated similarly to those for $GaAs_{1-x}N_x$ in Eq. (1). It should be noted that the lattice parameter of $Ga_{108}Sb_{107}N_{Sb}$ is interpolated using the lattice parameters of bulk GaSb, $Ga_{64}Sb_{63}N_{Sb}$, and $Ga_{32}Sb_{31}N_{Sb}$ systems.

For the bulk band gap of GaSb, we obtain the value of 0.65 eV, i.e., a slightly smaller value than 0.72 eV given in Refs. 22 and 29 and obtained also using hybrid functionals.

TABLE II. Relative binding energies $E_{b,\text{rel}}$, lattice parameters a, and band gaps E_g of different nitrogen pair configurations in relaxed supercells for $GaSb_{1-x}N_x$ alloys.

Configuration	$E_{b,\text{rel}}$ (eV)	a (Å)	E_g (eV)
bulk $Ga_{32}Sb_{32}$	. . .	6.16	0.65
$Ga_{108}Sb_{107}N_{Sb}$	. . .	6.15	0.39
$Ga_{64}Sb_{63}N_{Sb}$	. . .	6.13	0.07
$Ga_{32}Sb_{31}N_{Sb}$	. . .	6.10	. . .
$Ga_{32}Sb_{31}(N_2)_{Sb}$	0.22	6.13	0.41
$Ga_{32}Sb_{30}(N_{Sb}N_{Sb})_{\text{near}}$	−0.51	6.05	0.03
$Ga_{32}Sb_{30}(N_{Sb}N_{Sb})_{\text{far}}$	0.15	6.05	. . .
$Ga_{32}Sb_{30}(N_{Sb}N_{Sb})_{100}$	0.05	6.04	0.14

With Ga d electrons treated as valence, our optimized lattice constant is 6.15 Å and the band gap 0.73 eV for bulk GaSb. Thus the difference in the calculated band gap, compared to Ref. 22, can be explained by the different treatment of the Ga d electrons. Qualitatively band structures are identical whether the Ga d electrons are treated as core or not. The experimental 0 K band gap given in literature is 0.81 eV.[30] Thus our value is quite close to the experimental one and much better than band gaps obtained using semilocal functionals that may give even negative values.[29] The obtained lattice parameter for bulk GaSb is 6.16 Å (the Ga-Sb bond length is 2.67 Å).

The relative binding energy for $Ga_{32}Sb_{31}(N_2)_{Sb}$ in Table II is given in Sb-rich growth conditions. The obtained limits for the chemical potential μ_{Sb} of the Sb atom are -5.59 eV $\leqslant \mu_{Sb} \leqslant -5.13$ eV corresponding to Ga-rich and Sb-rich growth conditions, respectively. The values are obtained using the $R\bar{3}m$ structure of the bulk Sb. According to Table II, formation of a N_2 dimer by merging two substitutional N atoms is thermodynamically favored in GaSb in Sb-rich growth conditions in contrast to GaAs. The reason for this is the larger size of the Sb atom compared to As atom and thus the N_2 dimer fits better on the substitutional site compared to GaAs. However, the reaction kinetics, involving also an Sb atom filling the vacancy left by the other N atom, may hinder the N_2 dimer formation. The relative binding energies of the other nitrogen configurations show characteristics similar to GaAs, although the relative binding energies of these systems are smaller than in GaAs.

In the case of a single substitutional nitrogen atom in the 64-atom supercell, there are rather drastic differences compared to the corresponding case in GaAs. The nitrogen atom causes the band gap to vanish as can be deduced from the highly dispersive behavior of the two bands around the zero energy in Fig. 3(b). There is a large reduction of 51% in the volume of the surrounding Ga tetrahedron corresponding to the Ga-N bond length of 2.09 Å, which is very similar to that in the case of GaAs. Hence, in this sense, nitrogen is bound up with the same strength in both GaSb and GaAs. According to the DOS shown in Fig. 2(b), nitrogen induces well localized states at 0.9 eV above the VBM, similarly to the $Ga_{32}As_{31}N_{As}$ case. It is noteworthy that the distance between the CBM and the nitrogen-related states is nearly the same in both materials. Thus nitrogen behaves not only qualitatively, but also quantitatively in a similar way in GaSb and GaAs. The nitrogen-induced states hybridize with the bulk states and form tails in the DOS with similar extents toward the band gap in both materials due to similar Ga-N bonds. The DOS tails enter to the bulk gap regions causing the observed band gap reductions. Figure 4 shows LDOS for GaSb at the nitrogen atom and at the nearest Ga and Sb atoms indicating that the nitrogen induced states are very localized at the Ga-N bonds. The inset shows that also the tail is very localized to the Ga-N bonds and how it slowly decays to zero. The main qualitative difference in the effect of nitrogen doping between GaAs and GaSb is that the band gap reduction is stronger in GaSb than in GaAs. Namely, a single nitrogen atom in the 64-atom GaAs supercell narrows the band gap by 0.39 eV (see Table I), whereas in a similar calculation for GaSb, the bulk band gap of 0.65 eV is eventually closed. Based on the above discussion, the main reason to this qualitative difference

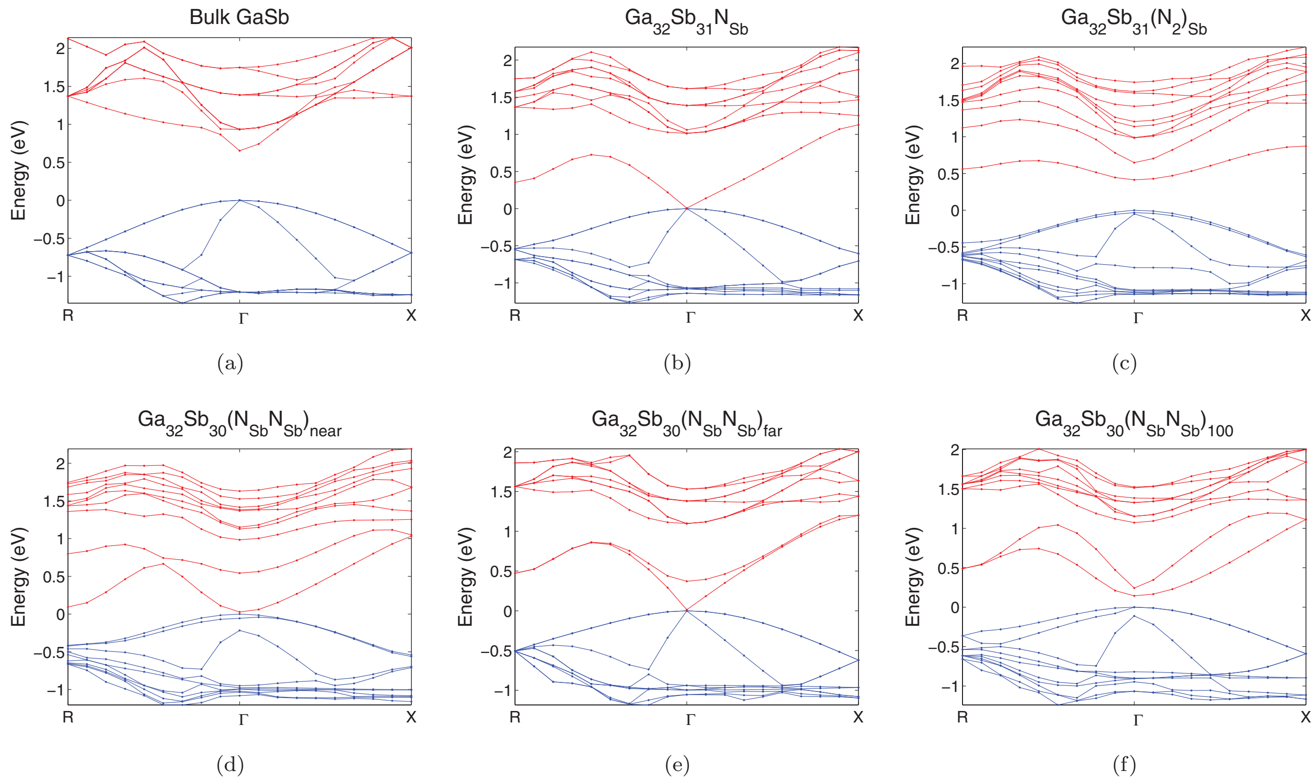

FIG. 3. (Color online) Band structures for the supercells of (a) bulk $Ga_{32}Sb_{32}$, (b) $Ga_{32}Sb_{31}N_{Sb}$, (c) $Ga_{32}Sb_{31}(N_2)_{Sb}$, (d) $Ga_{32}Sb_{30}(N_{Sb}N_{Sb})_{near}$, (e) $Ga_{32}Sb_{30}(N_{Sb}N_{Sb})_{far}$, and (f) $Ga_{32}Sb_{30}(N_{Sb}N_{Sb})_{100}$. The energy zero is defined to coincide with the top of the valence band.

is the strict positions of the nitrogen-induced states relative to the bulk CBM's, which determines how far into the bulk gap region the tail of the nitrogen-induced states extends. Our model can be supported by the following slightly qualitative arguments. According to Ref. 32, for GaAs and GaSb, CBM's are nearly at the same distance from the vacuum level. The energy levels of the localized Ga-N bond will lie at the same energy relative to the vacuum in both GaAs and in GaSb, meaning that also the distances between the nitrogen induced states and the bulk CBM's are similar. However, even small differences, e.g., in bulk CBM's between GaAs and GaSb relative to the vacuum, can lead to the observed stronger band gap reduction in $GaSb_{1-x}N_x$.

For the $Ga_{32}Sb_{31}(N_2)_{Sb}$ supercell, the results are similar to those for GaAs. The band gap is reduced from 0.65 to 0.41 eV and there is a 28% reduction in the volume of the tetrahedron surrounding the dimer. The conduction band edge becomes also clearly separated from the other bands and it is only slightly dispersed as in the case of GaAs. The conduction band edge results from the strong interaction of p electrons of the two nitrogen atoms, which have a localized state 0.75 eV above the VBM. In the case of two substitutional nitrogen atoms located in the far and (100) configurations in the 64-atom GaSb supercells, the local relaxations are again very similar to the corresponding cases in GaAs. The nitrogen atoms remain at the centers of Ga tetrahedra, and there is a 50% reduction in the volume surrounding the nitrogen atoms in both configurations. In the far configuration, the band gap vanishes similarly to the case of the single substitutional nitrogen atom. However, in the (100) configuration, the band gap opens, resembling the corresponding GaAs case, to 0.14 eV. Also the DOS in the far and (100) configurations, given in Fig. 2(b) show very similar characteristics to the corresponding cases in GaAs in Fig. 2(a). It seems that, even if the nitrogen atoms are not next-nearest neighbors in the far and (100) configurations, the nitrogen induced perturbations in the electronic structure begin to overlap, causing the observed rather unpredictable behavior of the band gap. In the case of two next-nearest neighbor nitrogen atoms, the band gap clearly opens, although to 0.03 eV

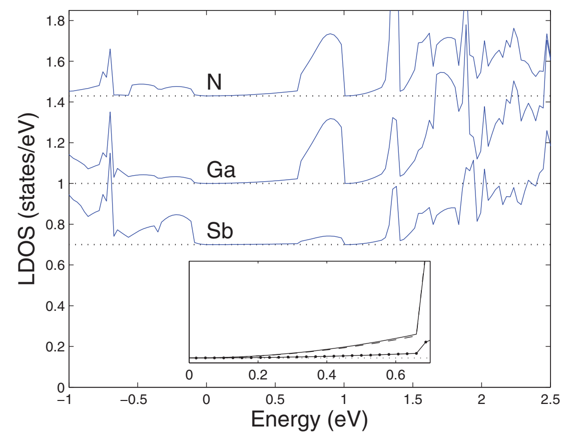

FIG. 4. (Color online) LDOS in the case of $Ga_{32}Sb_{31}N_{Sb}$ at the nitrogen atom and at the nearest gallium and antimony atoms. The inset figure shows the slow decay of the LDOS at nitrogen (solid line), gallium (dashed line), and antimony (dotted line). The dots indicate the zero level. The numbers on the vertical axis serve only as a scale.

only. This means a clearly different behavior compared to the corresponding case in GaAs where the band gap decreases by 0.19 eV when going from the far to the near configuration. However, the DOS is very similar to the corresponding case in GaAs and the nitrogen-induced states are split into two peaks. The splitting is related to the N-N interaction in the near configuration, causing the lower peak, when the upper peak is related to the bonding of nitrogen to the surrounding Ga atoms. In the far and (100) configurations, the minimum Ga-N bond length is 2.08 Å and in the near configuration 2.06 Å.

In Ref. 15, dilute nitride GaN_xSb_{1-x} alloys were studied in the TB framework. In that work, large 1728-atom supercells were used and the effect of randomly distributed nitrogen clusters to the band gap of GaSb was studied. The band gap was found to range from 0.1 to 0.3 eV with the concentration corresponding to a single substitutional nitrogen in the 64-atom supercell, depending on the configuration of the nitrogen atoms. However, also the bulk band gap, around 0.8 eV, was found to be clearly higher than our value and that is why it is reasonable to assume that the differences compared to Ref. 15 depend partly also on the parameters used in the tight-binding model. In Ref. 15, it was found that BAC model can only be used to describe isolated nitrogen atoms and that there is a certain distance above which the nitrogen atoms are efficiently independent.

Figure 5 shows the calculated band gap and lattice parameter as a function of the nitrogen concentration in GaSb. Also the experimental band gaps at room temperature as a function of nitrogen concentration, taken from Ref. 5, are shown. According to Fig. 5, the calculated band gap decreases strongly with the increasing nitrogen concentration showing a somewhat linear behavior at small concentrations. The lattice parameter decreases linearly, which is in consensus to experimental results for $GaAs_{1-x}N_x$ at small concentrations.[31] The behavior of the calculated band gap can be explained as follows. In the case of nearly isolated nitrogen atoms, the positions of the nitrogen-induced states are independent of the nitrogen concentration, but the extent of the tail of these states increases rapidly with increasing nitrogen concentration, causing the observed rapid band gap reduction at small concentrations. This was also observed in the band structures

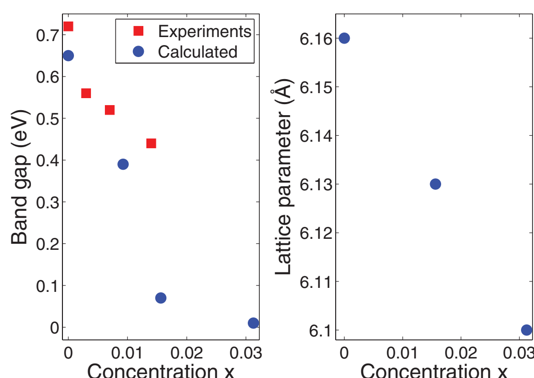

FIG. 5. (Color online) Band gaps and lattice parameters of $GaSb_{1-x}N_x$ alloys as a function of the nitrogen concentration. The experimental values are taken from Ref. 5 and are measured at the room temperature.

of Ref. 15. When the nitrogen concentration still increases, the extent of the tail of the nitrogen-induced states starts to saturate causing band gap freezing. However, the plotted experimental band gaps may show an earlier saturation of the band gap narrowing (the data point at $x = 0.014$) than the calculated ones. An obvious reason is the fact that the calculated band gaps are based on idealized periodic structures with a single nitrogen atom. In actual GaSb layers, the nitrogen atoms are not necessarily all on substitutional sites and one cannot rule out the formation of substitutional N_2 dimers, which reduce the band gap only moderately as discussed above, or the formation of larger nitrogen clusters, as was shown in Ref. 11.

IV. CONCLUSIONS

In this work, *ab initio* band structures of different nitrogen configurations were calculated for $GaAs_{1-x}N_x$ and $GaSb_{1-x}N_x$ alloys using the HSE06 hybrid functional. In addition, the band gaps of $GaSb_{1-x}N_x$ alloys were studied as a function of nitrogen concentration.

It was found that the effect of nitrogen can be described qualitatively correctly in GaAs using the HSE06 functional, giving a clear improvement in the relative band gap reduction compared to the (semi)local functionals in which the band gap nearly vanishes when nitrogen is added. Especially, the used hybrid functional shows its strength in describing $GaSb_{1-x}N_x$ alloys in which the band gap completely vanishes when using (semi)local functionals. In contrast, hybrid functionals make the comparison between $GaSb_{1-x}N_x$ and $GaAs_{1-x}N_x$ *ab initio* possible. It was found that nitrogen affects both GaAs and GaSb in a similar way, by creating well localized states above the band gap, related to the bonding of nitrogen to the surrounding Ga atoms.

The clustering of nitrogen atoms was found to lead to a clearly different concentration dependence compared to the case of more isolated nitrogen atoms, in such a way that the band gap does not systematically decrease with the increasing nitrogen concentration. The possible reason is the overlap of the nitrogen-induced perturbations in the electronic structure. By comparing the calculated band gaps corresponding to different nitrogen concentrations to the experimental values, it was found that these behave similarly at small concentrations. However, at larger nitrogen concentrations, the calculated band gaps drop much faster compared to experiments. The most likely reason to this is the possible clustering of nitrogen atoms in experiments, which leads to a different dependence of band gap on nitrogen concentration. Especially, formation of N_2 dimers is favorable in GaSb in Sb-rich growth conditions, which have a completely different effect on the band structure of GaSb compared to more isolated nitrogen atoms.

According to our calculations, in the case of a single nitrogen atom in the supercell, the tail in DOS due to the nitrogen-induced states hybridizes with bulk conduction band states and extends toward the band gap by the same amount in both materials. This is due to similar Ga-N bonds. The tails enter into the bulk band gap regions causing the observed band gap reductions. The reason for the observed stronger band gap reduction in $GaSb_{1-x}N_x$ than in $GaAs_{1-x}N_x$ was

found to be the positions of bulk band edges relative to the Ga-N bond energy, i.e., the position of the nitrogen induced states. Our findings do not support the common suggestion that the greater electronegativity mismatch between N and Sb compared to that between N and As should explain the stronger band gap reduction in $GaSb_{1-x}N_x$ than in $GaAs_{1-x}N_x$.

ACKNOWLEDGMENTS

This work has been supported by the Academy of Finland through the Center of Excellence program. The computer time was provided by the Finnish IT Center for Science and Technology (CSC).

[1] J. W. Ager III and W. Walukiewicz, Semicond. Sci. Technol. **17**, 741 (2002).
[2] E. P. O'Reilly, A. Lindsay, P. J. Klar, A. Polimeni, and M. Capizzi, Semicond. Sci. Technol. **24**, 033001 (2009).
[3] M. Weyers, M. Sato, and H. Ando, Jpn. J. Appl. Phys. **31**, 853 (1992).
[4] T. D. Veal, L. F. J. Piper, S. Jollands, B. R. Bennett, P. H. Jefferson, P. A. Thomas, C. F. McConville, B. N. Murdin, L. Buckle, G. W. Smith, and T. Ashley, Appl. phys. Lett. **87**, 132101 (2005).
[5] D. Wang, S. P. Svensson, L. Shterengas, G. Belenky, C. S. Kim, I. Vurgaftman, and J. R. Meyer, J. Appl. Phys. **105**, 014904 (2009).
[6] P. H. Jefferson, T. D. Veal, L. F. J. Piper, B. R. Bennet, C. F. McConville, B. N. Murdin, L. Buckle, G. W. Smith, and T. Ashley, Appl. phys. Lett. **89**, 111921 (2006).
[7] *Comparison of the Electronic Band Formation and Band Structure of GaNAs and GaNP in Dilute III-V Nitride Semiconductors and Material Systems*, edited by A. Erol (Springer, Berlin, 2008).
[8] W. Shan, W. Walukiewicz, J. W. Ager III, E. E. Haller, J. F. Geisz, D. J. Friedman, J. M. Olson, and S. R. Kurtz, Phys. Rev. Lett. **82**, 1221 (1999).
[9] P. R. C. Kent, L. Bellaiche, and A. Zunger, Semicond. Sci. Technol. **17**, 851 (2002).
[10] A. Lindsay and E. P. O'Reilly, Phys. Rev. Lett. **93**, 196402 (2004).
[11] L. Ivanova, H. Eisele, M. P. Vaughan, Ph. Ebert, A. Lenz, R. Timm, O. Schumann, L. Geelhaar, M. Dähne, S. Fahy, H. Riechert, and E. P. O'Reilly, Phys. Rev. B **82**, 161201 (2010).
[12] E. P. O'Reilly, A. Lindsay, S. Tomic, and M. Kamal-Saadi, Semicond. Sci. Technol. **17**, 870 (2002).
[13] E. P. O'Reilly and A. Lindsay, J. Phys.: Conference Series **242**, 012002 (2010).
[14] X. Liu, M. -E. Pistol, L. Samuelson, S. Schwetlick, and W. Seifert, Appl. phys. Lett. **56**, 1451 (1990).
[15] A. Lindsay, E. P. O'Reilly, A. D. Andreev, and T. Ashley, Phys. Rev. B **77**, 165205 (2008).
[16] P. Carrier, S.-H. Wei, S. B. Zhang, and S. Kurtz, Phys. Rev. B **71**, 165212 (2005).
[17] E. Arola, J. Ojanen, H.-P. Komsa, and T. T. Rantala, Phys. Rev. B **72**, 045222 (2005).
[18] K. Laaksonen, H.-P. Komsa, T. T. Rantala, and R. M. Nieminen, J. Phys. Condens. Matter **20**, 235231 (2008).
[19] J. E. Lowther, S. K. Estreicher, and H. Temkin, Appl. phys. Lett. **79**, 200 (2001).
[20] K. Laaksonen, H.-P. Komsa, E. Arola, T. T. Rantala, and R. M. Nieminen, J. Phys. Condens. Matter **18**, 10097 (2006).
[21] A. Belabbes, M. Ferhat, and A. Zaoui, Appl. phys. Lett. **88**, 152109 (2006).
[22] J. Heyd, J. E. Peralta, and G. E. Scuseria, J. Chem. Phys. **123**, 174101 (2005).
[23] G. Kresse and J. Furthmüller, Comput. Mater. Sci. **6**, 15 (1996).
[24] G. Kresse and D. Joubert, Phys. Rev. B **59**, 1758 (1999).
[25] J. P. Perdew, M. Ernzerhof, and K. Burke, J. Chem. Phys. **105**, 9982 (1996).
[26] A. Peles, A. Janotti, and C. G. Van de Walle, Phys. Rev. B **78**, 035204 (2008).
[27] J. E. Peralta, J. Heyd, G. E. Scuseria, and R. L. Martin, Phys. Rev. B **74**, 073101 (2006).
[28] C. G. Van de Walle and J. Neugebauer, J. Appl. Phys. **95**, 3851 (2004).
[29] Y.-S. Kim, M. Marsman, G. Kresse, F. Tran, and P. Blaha, Phys. Rev. B **82**, 205212 (2010).
[30] I. Vurgaftman, J. R. Meyer, and L. R. Ram-Mohan, J. Appl. Phys. **89**, 5815 (2001).
[31] S. G. Spruytte, C. W. Coldren, J. S. Harris, W. Wampler, P. Krispin, K. Ploog, and M. C. Larson, J. Appl. Phys. **89**, 4401 (2001).
[32] C. G. Van de Walle and J. Neugebauer, Nature (London) **423**, 626 (2003).